3. Chen YC, Hsu WY, Chang TH. Macrolide-resistant *Mycoplasma pneumoniae* infections in pediatric community-acquired pneumonia. Emerg Infect Dis. 2020;26:1382–91. https://doi.org/10.3201/eid2607.200017
4. Yamazaki T, Kenri T. Epidemiology of *Mycoplasma pneumoniae* infections in Japan and therapeutic strategies for macrolide-resistant *M. pneumoniae.* Front Microbiol. 2016;7:693.https://doi.org/10.3389/fmicb.2016.00693
5. Hieu Vy NT. Children with increased *Mycoplasma* pneumonia, instructions for disease prevention [in Vietnamese] [cited 2023 Jun 26]. https://benhviennhitrung-guong.gov.vn/tre-mac-viem-phoi-do-mycoplasma-gia-tang-huong-dan-phong-benh.html
6. Thompson JD, Higgins DG, Gibson TJ. CLUSTAL W: improving the sensitivity of progressive multiple sequence alignment through sequence weighting, position-specific gap penalties and weight matrix choice. Nucleic Acids Res. 1994;22:4673–80.
7. Sweeney BA, Hoksza D, Nawrocki EP, Ribas CE, Madeira F, Cannone JJ, et al. R2DT is a framework for predicting and visualising RNA secondary structure using templates. Nat Commun. 2021;12:3494. https://doi.org/10.1038/s41467-021-23555-5
8. Kim JH, Kim JY, Yoo CH, Seo WH, Yoo Y, Song DJ, et al. Macrolide resistance and its impacts on *M. pneumoniae* pneumonia in children: comparison of two recent epidemics in Korea. Allergy Asthma Immunol Res. 2017;9:340–6. https://doi.org/10.4168/aair.2017.9.4.340
9. Lucier TS, Heitzman K, Liu SK, Hu PC. Transition mutations in the 23S rRNA of erythromycin-resistant isolates of *Mycoplasma pneumoniae.* Antimicrob Agents Chemother. 1995;39:2770–3. https://doi.org/10.1128/AAC.39.12.2770
10. Matsuoka M, Narita M, Okazaki N, Ohya H, Yamazaki T, Ouchi K, et al. Characterization and molecular analysis of macrolide-resistant *Mycoplasma pneumoniae* clinical isolates obtained in Japan. Antimicrob Agents Chemother. 2004;48:4624–30. https://doi.org/10.1128/AAC.48.12.4624-4630.2004

Address for correspondence: Huyen Thi Thanh Tran, Medical Genetics Department, Vinmec High Tech Center, 458 Minh Khai, Hai Ba Trung Hanoi 100000, Vietnam; email: v.huyenttt47@vinmec.com

Crimean-Congo Hemorrhagic Fever Virus in Ticks Collected from Cattle, Corsica, France, 2023

Paloma Kiwan, Shirley Masse, Geraldine Piorkowski, Nazli Ayhan, Morena Gasparine, Laurence Vial, Remi N. Charrel, Xavier de Lamballerie, Alessandra Falchi

Author affiliations: Unité des Virus Emergents, Aix Marseille Université, Università di Corsica, IRD140, INSERM 207 IRBA, Marseille, France (P. Kiwan, S. Masse, G. Piorkowski, N. Ayhan, M. Gasparine, R.N. Charrel, X. de Lamballerie, A. Falchi); Université de Corse–Institut National de Santé et de la Recherche Médicale, Corte, France (P. Kiwan, S. Masse, G. Piorkowski, N. Ayhan, M. Gasparine, R.N. Charrel, X. de Lamballerie, A. Falchi); Centre National de Référence des Arbovirus, Marseille, France (N. Ayhan, X. de Lamballerie); Université de Montpellier, Montpellier, France (L. Vial)

We report the detection of Crimean-Congo hemorrhagic fever virus (CCHFV) in Corsica, France. We identified CCHFV African genotype I in ticks collected from cattle at 2 different sites in southeastern and central-western Corsica, indicating an established CCHFV circulation. Healthcare professionals and at-risk groups should be alerted to CCHFV circulation in Corsica.

DOI: https://doi.org/10.3201/eid3005.231742

Crimean-Congo hemorrhagic fever (CCHF) is a tickborne disease caused by CCHF virus (CCHFV) (species *Orthonairovirus haemorrhagiae*, genus *Orthonairovirus,* family *Nairoviridae*, order *Bunyavirales*). Endemic in Africa, the Middle East, Asia, and Eastern Europe, CCHF has expanded to Western Europe (*1*). Repeated detection of CCHFV in Spain (*2*) raises questions about its circulation in neighboring countries, such as Portugal, Italy, and France.

In Corsica, a French Mediterranean island, a seroprevalence study of CCHFV conducted in livestock (cattle, goats, and sheep) during 2014–2016 showed an overall seroprevalence of 9.1%, and cattle harbored the highest rates (*3*). A subsequent surveillance study of 8,051 ticks collected from wild (wild boar, deer, and mouflon sheep) and domestic (cattle, horses, sheep) animals during 2016–2020 failed to detect CCHFV or nairovirus RNA (*4*).

Since 2022, we have continued CCHFV surveillance by collecting ticks from cattle at 2 slaughterhouses ≥2 times/month. Cattle originate from a broad

geographic area, and the national ear-tag identification system enables tracing of each animal's origin and farm owner (Figure). We identified ticks by using taxonomic keys, then pooled ticks by species, sex, development stage, study site, and animal host, as previously reported (*4*). We spiked each pool, consisting of 1–6 ticks, with a predefined amount of MS2 bacteriophage for monitoring nucleic acid extraction, reverse transcription PCR (RT-PCR), and nucleic acid amplification (*5*). We used MagMAX Viral/Pathogen Ultra Nucleic Acid Isolation Kit (Thermo Fisher Scientific, https://www.thermofisher.com) to purify nucleic acids. We tested each sample by using 2 real-time RT-PCRs, 1 targeting the large (L) RNA segment (*2*) and 1 targeting the small (S) RNA segment (*6*). We used the SuperScript IV One-Step RT-PCR System Kit (ThermoFisher) to design 28 CCHFV-specific pairs of primers to amplify the S, medium (M), and L segments (Appendix, https://wwwnc.cdc.gov/EID/article/30/5/23-1742-App1.pdf). We sequenced PCR products by using S5 Ion Torrent technology (ThermoFisher). We determined the best model by using the maximum-likelihood method and performed phylogenetic analyses by using MEGA6 software (*7*) (Figure).

During June 2022–July 2023, we collected 5,165 ticks from 465 cattle and grouped ticks into 1,491 pools. Tick species consisted of 2,390 (46.27%) *Rhipicephalus bursa*, 1,103 (21.35%) *Hyalomma marginatum*, 750 (14.52%) *Boophilus annulatus*, 507 (9.81%) *Hyalomma scupense*, 238 (4.60%) *Haemaphysalis punctata*, 127 (2.45%) *Ixodes ricinus*, 48 (0.92%) *Rhipicephalus*

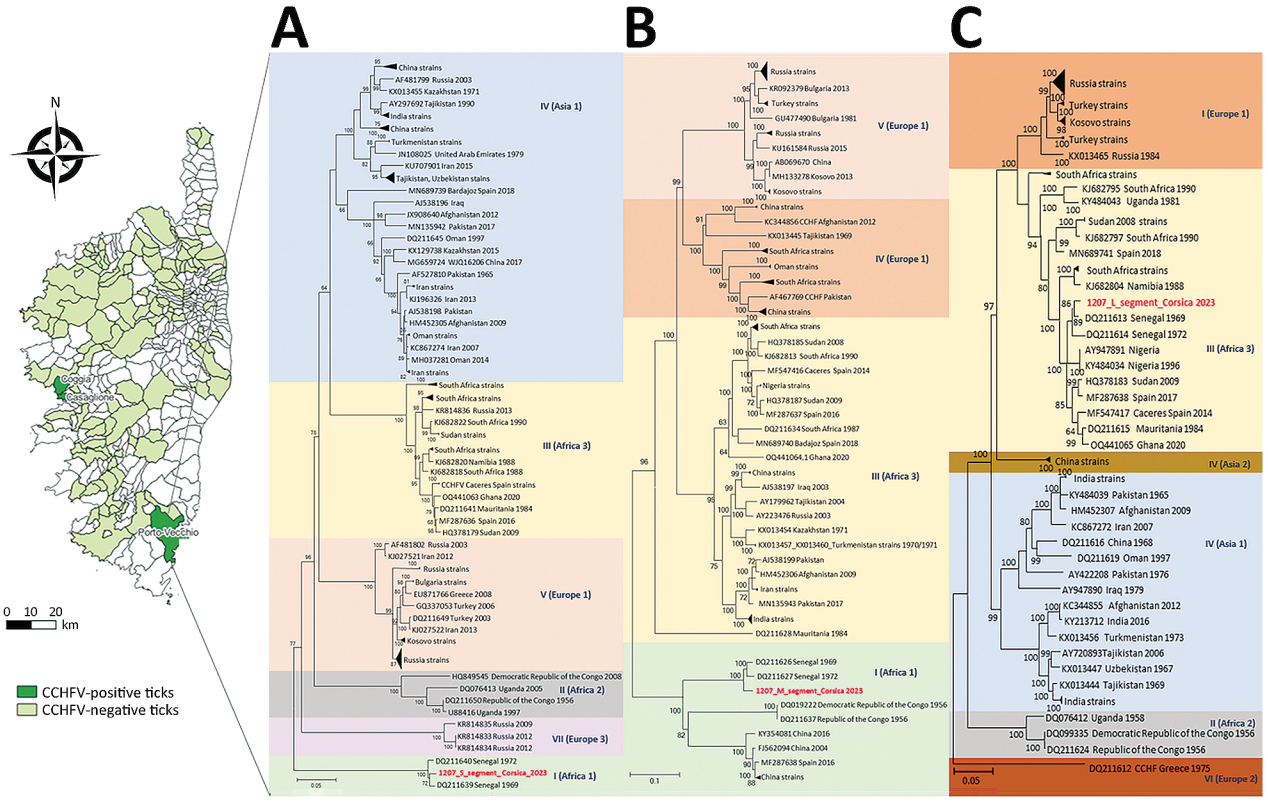

Figure. Phylogenetic analysis of Crimean-Congo hemorrhagic fever virus in ticks collected from cattle, Corsica, France, 2023. Map at left shows locations of cattle from which ticks were collected at the slaughterhouses of Ponte Leccia in the north and Cuttoli-Corticchiatto in the south during 2022–2023. Phylogenetic trees show small (A), medium (B), and large (C) RNA segments CCHFV strains. Red font indicates strains detected from Corsica; other sequences are named by GenBank accession number, geographic origin, and sampling year. Evolutionary analyses were conducted in MEGA6 (https://www.megasoftware.net) after best model determination. The optimal tree is shown for each fragment. Trees were constructed using the maximum-likelihood method based on sequences on the small (Tamura-Nei model), medium (general time-reversible model), and large (Tamura-Nei model) segments of the virus. All positions with <95% sequence site coverage were eliminated (i.e., <5% alignment gaps, missing data, or ambiguous bases were allowed at any position [partial deletion option]). Results of bootstrap test (1,000 replicates) are shown next to the branches. Genotypes are indicated by Roman numerals (*8*) with the equivalent clade nomenclature (*9*): I, West Africa (Africa 1); II, Central Africa (Africa 2); III, South and West Africa (Africa 3); IV, Middle East/Asia, divided into 2 groups Asia 1 and Asia 2; V (Europe 1), Europe/Turkey (Europe 1); VI, Greece (Europe 2); VII (Europe 3). Scale bars indicate nucleotide substitutions per site. CCHFV, Crimean-Congo hemorrhagic fever virus; L-RNA, large segment of CCHFV RNA.

Table. Description of Crimean-Congo hemorrhagic fever virus in tick pools collected from cattle, Corsica, France, 2023*

Cattle ID nos.	Cattle origin	Collection date	CCHFV–positive pool nos.	CCHFV assay, Ct		Tick species	Tick sex	No. ticks per pool
				L segment	S segment			
2478	Coggia	2022 Sep 27	417	IND	IND	*Haemaphysalis punctata*	F	1
6069	Coggia	2022 Sep 27	418	IND	IND	*H. punctata*	M	1
4376	Casaglione	2023 May 9	1252	IND	IND	*Rhipicephalus bursa*	M	6
			1253	IND	IND	*R. bursa*	M	6
4371	Casaglione	2023 May 9	1233	40.8	IND	*Hyalomma marginatum*	M	6
4039	Porto-Vecchio	2023 May 9	1204	35.9	IND	*R. bursa*	M	6
			1205	34.7	IND	*R. bursa*	F	6
			1206	34	IND	*R. bursa*	F	6
			1207	31.9	40	*R. bursa*	M	6
			1208	34.2	IND	*R. bursa*	M	6
			1209	33.7	IND	*R. bursa*	F	6
			1210	33.5	IND	*R. bursa*	M	6
			1211	32.9	IND	*Hyalomma marginatum*	M	6
			1212	34.7	40	*R. bursa*	M	6
			1213	33.2	IND	*Hyalomma marginatum*	F	6
			1214	33.1	IND	*R. bursa*	F	6
			1215	33.8	IND	*R. bursa*	F	6
			1218	34.2	IND	*Hyalomma marginatum*	M	4
			1219	35	IND	*Hyalomma marginatum*	F	6
			1220	35.1	IND	*Hyalomma marginatum*	M	3
			1221	34.1	IND	*R. bursa*	M	6
			1222	36.5	IND	*R. bursa*	M	6
			1223	35.7	IND	*Rhipicephalus sanguineus*	M	1
			1224	37.5	IND	*R. bursa*	F	1
Total			24 pools					119

*Pools of ticks were tested with quantitative reverse transcription PCR of the L and S segments of CCHFV RNA. A total of 24 pools comprising 119 ticks were tested CCHFV-positive from 5 animals. CCHFV, Crimean-Congo hemorrhagic fever virus; Ct, cycle threshold; ID, identification; IND, indeterminate (weakly positive); L, large; S, small.

sanguineus, and 2 (0.03%) *Dermacentor marginatus*. A total of 24 (1.70%) pools collected from 5 cattle from southern Corsica tested positive by the L-RNA assay (Table). Nineteen of the 24 tick pools were collected from 1 animal (no. 4039) (Table). Partial sequences for S (1,340 bp), M (4,894 bp), and L (11,275 bp) segments were obtained from animal nos. 2478 (pool 417) and 4039 (pool 1207) (Table). The effective detection of CCHFV genome is strongly supported by the formal exclusion of contamination because no CCHFV strain or genome had been previously processed in the laboratory, the PCR systems used can distinguish genomic RNA from the positive control (*6*), and the CCHFV sequences obtained were original and unambiguous.

The obtained S and M segment sequences constituted a monophyletic group belonging to genotype I (Africa 1), whereas the L segment sequence grouped with genotype III strains (Africa 3) (Figure). The sequences of all 3 segments of the CCHFV from Corsica are closely related to 2 sequences from Senegal corresponding to strains identified in the 1970s and likely represent strains reassorted in Senegal. Whether those strains are typical of strains from Senegal or have been circulating in other parts of Africa requires additional investigations.

Our results suggest that CCHFV strains circulating in Corsica and Spain have distinct origins. In Spain, genotype III is the most widespread and is most often detected in *H. lusitanicum* ticks (*2*), a species not yet identified in Corsica. Trans-Saharan migratory birds carrying *H. marginatum* ticks are the most likely source of CCHFV strains entering Corsica (*6*). Examination of the main bird migration routes suggests that 2 different migratory corridors link Spain and Corsica to Africa; mainly, but not exclusively, West Africa for Spain and Central Africa for Corsica (*6*). Those migration routes also could explain the different origin of CCHFV strains circulating in Corsica and in Spain.

Our results provide evidence for established CCHFV circulation in Corsica because detection occurred at 2 distinct sites in the southeastern and central western parts of the island. In addition, our results provide evidence for infection in cattle because multiple CCHFV-positive ticks were found on the same animal. CCHFV detection in feeding ticks is indicative of virus circulation within the cattle population but does not elucidate the role of ticks in virus transmission. Our results must be interpreted by considering previous serologic evidence of CCHFV circulation in cattle in Corsica (*3*), the presence of competent vectors locally (*4*), and recent reports of CCHFV detection in southern mainland France (*10*). The threat of possible continuous expansion and circulation of the virus over Western Europe should not be disregarded. Healthcare professionals and other groups at risk for infection, including hunters and farmers, should be informed about CCHFV circulation in Corsica.

Acknowledgments

We thank the staff of the slaughterhouses for their help in collecting ticks from cattle. We thank Gregory Mollé, Laurence Thirion, Pierre Combe, and Cecile Baronti for the production and validation of diagnostic reagents.

This work was supported in part by the VHFMODRAD project (no. 823666, call H2020-JTI-IMI2-2015-08-single-stage) of the H2020 program by the Innovative Health Initiative (IHI) agency of the European Commission; by the European Commission European Virus Archive Global project (EVA GLOBAL, grant agreement no. 871029) of the Horizon 2020 Research and Innovation Programme; and by Centre de Coopération Internationale en Recherche Agronomique pour le Développement (provision of service no. E2F03F6F). The reagent material was provided by the European Virus Archive-Marseille (EVAM) under the label technological platforms of Aix-Marseille University.

About the Author

Ms. Kiwan is a PhD student at the Unité des Virus Emergents, University of Corsica Pascal Paoli and Aix-Marseille University, France. Her primary research interests focus on tickborne viruses via a One Health approach.

References

1. Lorenzo Juanes HM, Carbonell C, Sendra BF, López-Bernus A, Bahamonde A, Orfao A, et al. Crimean-Congo hemorrhagic fever, Spain, 2013–2021. Emerg Infect Dis. 2023;29:252–9. https://doi.org/10.3201/eid2902.220677
2. Sánchez-Seco MP, Sierra MJ, Estrada-Peña A, Valcárcel F, Molina R, de Arellano ER, et al.; Group for CCHFv Research. Widespread detection of multiple strains of Crimean-Congo hemorrhagic fever virus in ticks, Spain. Emerg Infect Dis. 2021;28:394–402. https://doi.org/10.3201/eid2802.211308
3. Grech-Angelini S, Lancelot R, Ferraris O, Peyrefitte CN, Vachiery N, Pédarrieu A, et al. Crimean-Congo hemorrhagic fever virus antibodies among livestock on Corsica, France, 2014–2016. Emerg Infect Dis. 2020;26:1041–4. https://doi.org/10.3201/10.3201/eid2605.191465
4. Cicculli V, Maitre A, Ayhan N, Mondoloni S, Paoli JC, Vial L, et al. Lack of evidence for Crimean-Congo hemorrhagic fever virus in ticks collected from animals, Corsica, France. Emerg Infect Dis. 2022;28:1035–8. https://doi.org/10.3201/eid2805.211996
5. Ninove L, Nougairede A, Gazin C, Thirion L, Delogu I, Zandotti C, et al. RNA and DNA bacteriophages as molecular diagnosis controls in clinical virology: a comprehensive study of more than 45,000 routine PCR tests. PLoS One. 2011;6:e16142. https://doi.org/10.1371/journal.pone.0016142
6. Estrada-Peña A, D'Amico G, Fernández-Ruiz N. Modelling the potential spread of *Hyalomma marginatum* ticks in Europe by migratory birds. Int J Parasitol. 2021;51:1–11. https://doi.org/10.1016/j.ijpara.2020.08.004
7. Tamura K, Stecher G, Peterson D, Filipski A, Kumar S. MEGA6: Molecular Evolutionary Genetics Analysis version 6.0. Mol Biol Evol. 2013;30:2725–9. https://doi.org/10.1093/molbev/mst197
8. Chamberlain J, Cook N, Lloyd G, Mioulet V, Tolley H, Hewson R. Co-evolutionary patterns of variation in small and large RNA segments of Crimean-Congo hemorrhagic fever virus. J Gen Virol. 2005;86:3337–41. https://doi.org/10.1099/vir.0.81213-0
9. Carroll SA, Bird BH, Rollin PE, Nichol ST. Ancient common ancestry of Crimean-Congo hemorrhagic fever virus. Mol Phylogenet Evol. 2010;55:1103–10. https://doi.org/10.1016/j.ympev.2010.01.006
10. Anses – National Agency for Food, Environmental and Occupational Health Safety. Crimean-Congo hemorrhagic fever: first detection of the virus in cattle farms in southern France [in French] [cited 2023 Dec 18]. https://www.anses.fr/fr/content/fievre-hemorragique-crimee-congo-detection-virus-elevages-bovins

Address for correspondence: Alessandra Falchi, Unité des Virus Emergents, IRD 190-Inserm 1207, University of Corsica Pascal Paoli and Aix-Marseille University, Laboratoire de Virologie, Faculté des Sciences, Campus Grimaldi, Corte 20250, France; email: falchi_a@univ-corse.fr

Deforestation and Bovine Rabies Outbreaks in Costa Rica, 1985–2020

Christie Jones, Amanda Vicente-Santos, Julie A. Clennon, Thomas R. Gillespie

Author affiliation: Emory University, Atlanta, Georgia, USA

DOI: https://doi.org/10.3201/eid3005.230927

In Latin America, rabies virus has persisted in a cycle between *Desmodus rotundus* vampire bats and cattle, potentially enhanced by deforestation. We modeled bovine rabies virus outbreaks in Costa Rica relative to land-use indicators and found spatial-temporal relationships among rabies virus outbreaks with deforestation as a predictor.

Costa Rica has benefited from effective vaccination campaigns to eliminate canine rabies virus infections. Still, the virus has endured, spread by vampire bats (*Desmodus rotundus*) to cattle, with rare but documented transfer from bats to humans (*1*,*2*). To determine how anthropogenic disturbance affects

Article DOI: https://doi.org/10.3201/eid3005.231742

Crimean-Congo Hemorrhagic Fever Virus in Ticks Collected from Cattle, Corsica, France, 2023

Appendix

Appendix Table 1. System 1 for small (S) segment

Name	Sequence	Couple	Position
CrCon1 S	RWA-AYG-GRC-TTR-TGG-AYA-CYT-TCA-C-	Couple 1	123–147
CrCon1 R	TRG-CAA-GRC-CKG-TWG-CRA-CWA-GWG-C		764–740
CriCon2 S	ART-GGA-GRA-ARG-AYA-TWG-GYT-TYC-G	Couple 2	450–474
CriCon2 R	CYTTGA-YRA-AYT-CYC-TRC-ACC-ABT-C		674–650

Appendix Table 2. System 2 for small (S) segment

Primer name	Sequence (5′-3′)	Couple	Amplification size, bp
GP_CCHF_seg S_1S	TCTCAAAGAAACACGTGCCGC	Couple 1	472
GP-CCHF-segS-472R	GCTGTGTTTGCATTGACACGG		
GP-CCHF-segS-444S	GCCAATTACCAACARGCTGC	Couple 2	463
GP-CCHF-segS-907R	AGAGTTCCTGGGCCTTAGTG		
GP-CCHF-segS-845S	CATAAGGACGAAGTTGACAGG	Couple 3	413
GP-CCHF-segS-1258R	TGAGCCCTGGGCTGCATCG		
GP-CCHF-segS-1204S	GCAGAATTAGTGAGATGGGTG	Couple 4	485
GP_CCHF_seg S_1689R	CGCACAGCCCTTTAAGTRTTT		

Appendix Table 3. System 3 for small (S) segment

Primer name	Sequence (5′-3′)	Couple	Amplification size, bp
GP_CCHF_seg S_1S	TCTCAAAGAAACACGTGCCGC	Couple 1	1,689
GP_CCHF_seg S_1689R	CGCACAGCCCTTTAAGTRTTT		

Appendix Table 4. System 4 for medium (M) segment

Primer name	Sequence (5′-3′)	Couple	Amplification size, bp
GP-CCHF-segM-1Rbis	CTMTGYGAGAACAGTGCCWC	Couple 1	351
GP-CCHF-segM-351R	CTGGATTCACCAGAACCACTG		
GP-CCHF-segM-264S	CAATGTCTGTGCTGGAGTCAT	Couple 2	404
GP-CCHF-segM-668R	TGGTTGTGGTCATTACTGATGC		
GP-CCHF-segM-611S	GCACATCATCTCTCCAGAAG	Couple 3	450
GP-CCHF-segM-1061R	CTTGAACAGGCATGCAATGAC		
GP-CCHF-segM-987S	GCAAGATACTGAAACTCCTACA	Couple 4	476
GP-CCHF-segM-1463R	CATGGCAGTTTGAAAGATTAAC		
GP-CCHF-segM-1384S	CAACTGTATAAACTTGAAAGTGTC	Couple 5	479
GP-CCHF-segM-1863R	CTTTGATCCACTATTGTGGAGC		
GP-CCHF-segM-1842Sbis	AGCTATGGTGGKCCTGGYGARA	Couple 6	490
GP-CCHF-segM-2332R	AGTGTCCCGATGACAATTAGC		
GP-CCHF-segM-2296S	CATCACATGTGTAGTGTGCAAG	Couple 7	434
GP-CCHF-segM-2730R	CTCATTTGATAGACTTCAACTG		
GP-CCHF-segM-2692S	GTCACCAGTTCAGTCCGCA	Couple 8	469
GP-CCHF-segM-3161R	GTCGACAGCAGAGGTACTAAC		
GP-CCHF-segM-3084S	GCAACAGGGCTACTTTCATCA	Couple 9	403
GP-CCHF-segM-3487R	CCTGAAACTAAGATCTTGTTGC		
GP-CCHF-segM-3459S	CTTAGCTGGAGTTCAGTTGAAC	Couple 10	305
GP-CCHF-segM-3764Rbis	CGCCAGTTCCTCGAGTGCGGC		

Appendix Table 5. System 5 for medium (M) segment

Primer name	Sequence (5′-3′)	Couple	Amplification size, bp
GP_CCHF_seg M_1S	TCTCAAAGAAATACTTGCGGCAC	Couple 1	1,958
GP_CCHF_seg M_1959R	CCTGTGGCACTGTTTTCGCA		
GP_CCHF_seg M_1842S	AACTATGGTGGYCCRGGTGAYA	Couple 2	1,922
GP_CCHF_seg M_3764R	CTCCAGTTTCTTGARTGRGGC		
GP_CCHF_seg M_3711S	GAYTGCCCGGAAAGRTGTGG	Couple 3	1,855
GP_CCHF_seg M_5566R	TCTCAAAGATATAGTGGCGGC		
GP_CCHF_seg L_12211R	CCCCACACCCCAAAATAATAA		

Appendix Table 6. System 6 for large (L) segment

Primer name	Sequence (5′-3′)	Couple	Amplification size, bp
GP_CCHF_seg L_1S	TCTCAAAGATATCAATCCCCCC	Couple 1	415
GP-CCHF-segL-415S	GGCTAAAGAAATGGGCATTACC		
GP-CCHF-segL-459R	CTGCTTCCACTTCATCACTGG	Couple 2	405
GP-CCHF-segL-864R	GTGTCAGCTGATATCTCAACAC		
GP-CCHF-segL-819S	CCAGAGTCGGTAGAGTCTTG	Couple 3	480
GP-CCHF-segL-1299R	CACTGCAGACAGTTGCTAAGG		
GP-CCHF-segL-1251S	TTCTCGGCAACCTGGGAAATG	Couple 4	238
GP_CCHF_seg L_1489R	GAGATCAGCTATCTCCCTGTG		

Appendix Table 7. System 7 for large (L) segment

Primer name	Sequence (5′-3′)
GP-CCHF-segL-3732s	CTGTGCCAAGATCTTGGCTC
GP-CCHF-segL-4011R	GTGTCTACAATTCCCTCATAAG

Appendix Table 8. System 8 for large (L) segment

Primer name	Sequence (5′-3′)	Couple	Amplification size, bp
GP_CCHF_seg L_1S	TCTCAAAGATATCAATCCCCCC	Couple 1	1,488
GP_CCHF_seg L_1489R	GAGATCAGCTATCTCCCTGTG		
GP_CCHF_seg L_1259S	GYAACCTAGGAAATGAACTGTTG	Couple 2	1,708
GP_CCHF_seg L_2967R	CTTTGCGCATWGCCTGTTCC		
GP_CCHF_seg L_2809S	GTTGTTGGAGCYATAAGTACTC	Couple 3	1,605
GP_CCHF_seg L_4414R	GGARTGATTTTCAATGTCTTG		
GP_CCHF_seg L_4298S	AGGAGRCAAGCTGTCCTTGG	Couple 4	1,888
GP_CCHF_seg L_6178R	CTTTGACARTTCCAGRTGCTG		
GP_CCHF_seg L_6022S	CTCAACGAGCAACAAGATGAAC	Couple 5	1,584
GP_CCHF_seg L_7606R	CATGYTCAACATGTACTGTTGTC		
GP_CCHF_seg L_7491S	GYTACAACCATATGGGTCAGG	Couple 6	1,808
GP_CCHF_seg L_9299R	GCAGGTCTAGACTCAACTATTC		
GP_CCHF_seg L_9077S	CTCACTGGTTGGACACCTTTC	Couple 7	1,547
GP_CCHF_seg L_10624R	CTRTCTGTAGAGCAGTCMAC		
GP_CCHF_seg L_10253S	GTGARACTGAAAGRCAAGTGC	Couple 8	1,958
GP_CCHF_seg L_12211R	CCCCACACCCCAAAATAATAA		